AIAA JOURNAL
Vol. 44, No. 7, July 2006

Stability in a Twisted Periodic Blade System with Cracks

Bo-Wun Huang* and Huang-Kuang Kung†
Cheng Shiu University, Kaohsiung 833, Taiwan, Republic of China
and
Jao-Hwa Kuang‡
National Sun Yat-Sen University, Kaohsiung 804, Taiwan, Republic of China

DOI: 10.2514/1.15334

This paper investigates the variations in dynamic stability of a cracked rotating periodic bladed disk assembly. A bladed disk composed of periodically shrouded blades is used to simulate the coupled periodic structure. To study mode localization, a number of apparently identical blades are distributed periodically around a rigid hub. For simplicity, the rigid hub is considered to be attached to a rigid shaft. The modal localization equations of the rotating cracked assembly are formulated using Hamilton's principle and Galerkin's method. The regions of instability in this cracked assembly are identified by means of the multiple scales perturbation method. The numerical results indicate that the modal localization effect introduced by local blade cracks destabilizes the shrouded blade group. One additional instability band at the localization frequency is introduced from the local crack. Furthermore, it is shown that the stability regions of a cracked rotating bladed disk assembly are significantly dependent on the rotational speed, shroud stiffness, and crack depth.

Nomenclature

A	=	cross section area of the blade
a	=	depth of crack
b_0	=	width at the root of blade
b_1	=	width at the tip of blade
c. c.	=	complex conjugate
E	=	Young's modulus
F_j	=	magnitude of the perturbation speed
F_M	=	maximum of components of F_j
$f(t)$	=	variation of the rotation speed
k_s	=	shroud stiffness
L	=	length of the blade
N	=	total number of blades
P_b	=	bending moment at crack
p^*	=	centrifugal force
$p_i^s(t)$, $q_i^s(t)$	=	determined coefficients
R_h	=	root diameter of the turbodisk
r_c	=	position of the coupled shroud
r^*	=	position of the crack
s	=	number of blade
t_0	=	thickness at the root of blade
t_1	=	thickness at the tip of blade
U_s^k	=	strain energy stored in the sth shroud
U_s^e, U_s^Ω	=	strain energy introduced by the bending moment and the centrifugal force
u_s, v_s	=	deflections of the sth blade
u_ξ, v_ξ	=	deflections of the cracked blade
ε	=	perturbation parameter
$\phi_i^s(r)$	=	comparison functions, $i = 1, 2, \ldots$
λ_i	=	coefficients
μ	=	Poisson's ratio
θ	=	pretwist angle of the blade
ρ	=	density of the blade
Ω	=	rotation speed of the disk
Ω_0	=	steady rotational speed
ω	=	exciting frequency
ω_j	=	perturbation frequency
ω_0, ω_n	=	reference and natural frequencies

Received 30 December 2004; revision received 3 February 2006; accepted for publication 4 March 2006.

*Professor, Department of Mechanical Engineering, No. 840 Cheng Ching Rd., Niaosung; huangbw@csu.edu.tw.
†Professor, Department of Mechanical Engineering, No. 840 Cheng Ching Rd., Niaosung; hkkung@csu.edu.tw.
‡Corresponding Author, Professor, Department of Mechanical Engineering, No. 70 Lien-hai Rd.; kuang@mail.nsysu.edu.tw.

I. Introduction

CRACKS frequently appear in rotating machinery due to manufacturing flaws or cyclic fatigue during operation. In turbodisks particularly, numerous cracks can be observed following severe operating conditions [1,2]. Local structural irregularity, i.e., local disorder, caused by cracks on the blade, changes the dynamic behavior of a bladed disk assembly significantly. A number of researchers have investigated the modal localization phenomenon in weakly coupled periodic structures with local structural or material irregularities [3–8]. Such a phenomenon may in turn localize the vibration modes, thereby confining the vibration energy at the localization frequency.

A shrouded bladed disk can be regarded as a periodic system if all of its blades are assembled periodically. The dynamic behavior of such a bladed disk assembly has been studied by Cottney and Ewins [9], whereas the fundamental aspects of dynamic response in mistuned turbomachinery rotors have been studied by Afolabi et al. [10–12]. Furthermore, others [13,14] have studied the effect of local cracks on the mode localization phenomenon in various periodic systems. In considering the effect of local blade cracks on the dynamic behaviors of a turbodisk, the present study uses periodically coupled pretwisted beams to simulate the blades of the turbodisk. For simplicity, the tapered pretwisted beams are approximated as Euler-Bernoulli beams, as proposed previously by Rao [15,16]. During operational service, the rotational speed of a shrouded bladed disk is subject to slight variation as a result of external disturbance. Consequently, the parametric instability of a bladed disk assembly rotating with a nonconstant speed merits investigation. The majority of stability-orientated studies have been limited to tuned systems [17–20] within which no local disorder is evident. More recent articles [21–24] have investigated the stability of a rotating blade without or with a crack. By contrast, very few studies [25] have

considered dynamic stability issues in mistuned systems, especially for systems with cracks.

This study investigates the variation in dynamic stability of a bladed disk assembly with a cracked blade. Shrouded pretwisted Euler-Bernoulli beams are used to approximate the blades. The Galerkin method is employed to derive the discrete modal localization equation of the mistuned system, whereas the multiple scales perturbation method is employed to specify the regions of instability.

II. Equations of Motion

Figure 1a presents a schematic illustration of a periodically shrouded blade assembly rotating with a speed of Ω. As in Wei et al. [5,6,25], the present study considers the blade assembly to consist of a rigid hub of radius R_h and a cyclic assembly of N coupled blades. Each blade is coupled with its neighbor through a shroud. The length of the cantilever beam is L and each blade is coupled by the shroud ring to the adjacent one at a position of r_c. Figure 1b shows the current approximation of an individual blade by means of a tapered pretwisted beam. The thickness and breadth at the root of the blade are given by t_0 and b_0, respectively. The transverse flexible deflections of the sth blade in the rotational and out-off rotational planes are denoted by components $v_s(r,t)$ and $u_s(r,t)$, respectively. The equations of motion of a blade with and without a local crack are derived in the sections that follow.

A. Blades Without Crack

From a consideration of bending vibration, the kinetic energy of the rotating sth blade can be expressed as

$$T_s = \frac{1}{2}\int_0^L \rho A\{[\dot{u}_s(r,t)]^2 + [\dot{v}_s(r,t)]^2 + [\Omega v_s(r,t)]^2\}\,\mathrm{d}r \quad (1)$$

The cross sectional area of the taper beam at position r is given by

$$A(r) = b_0 t_0\left(1-\alpha\frac{r}{L}\right)\left(1-\beta\frac{r}{L}\right) \quad (2)$$

and the taper angles are

$$\alpha = \frac{b_0 - b_1}{b_0}; \qquad \beta = \frac{t_0 - t_1}{t_0} \quad (3)$$

The total strain energy of the sth blade comprises three individual components, i.e.,

$$U_s = U_s^e + U_s^\Omega + U_s^k \quad (4)$$

where U_s^e, U_s^Ω, and U_s^k are the strain energy components introduced by the bending deformation, the centrifugal force, and the elastic deformation of the shroud, respectively. These strain energy components are defined as

$$U_s^e = \frac{1}{2}\int_0^L E[I_{yy}(u_s'')^2 + 2I_{xy}(u_s'')(v_s'') + I_{xx}(v_s'')^2]\,\mathrm{d}r \quad (5)$$

$$U_s^\Omega = \frac{1}{2}\int_0^L p^*[(u_s')^2 + (v_s')^2]\,\mathrm{d}r \quad (6)$$

$$U_s^k = \frac{k_{s+1}}{2}[v_{s+1}(r_c,t) - v_s(r_c,t)]^2 \quad (7)$$

where $p^*(r)$ and k_{s+1} are the centrifugal force and stiffness of the shroud ring, respectively, E is Young's modulus of the blade, and I_{xx}, I_{yy}, and I_{xy} are the area moments of the pretwisted blade.

The blade is pretwisted with a uniform twist angle of θ. Accordingly, the area moments at position r are given by

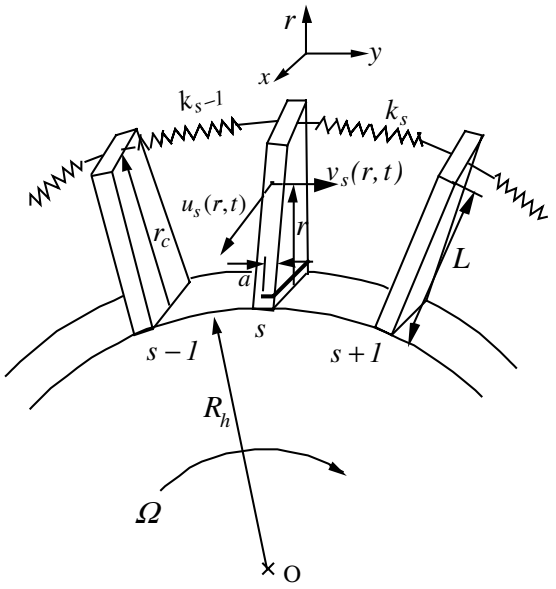

a)

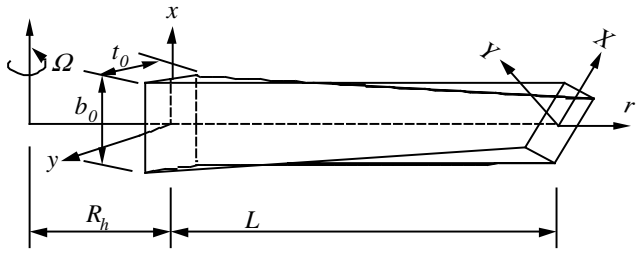

b)

Fig. 1 Geometry of cyclically arranged bladed disk assembly: a) geometry of bladed disk assembly, and b) geometry of pretwisted taper blade.

$$I_{xx}(r) = I_{XX}\cos^2\left(\frac{r}{L}\theta\right) + I_{YY}\sin^2\left(\frac{r}{L}\theta\right) \quad (8a)$$

$$I_{yy}(r) = I_{XX}\sin^2\left(\frac{r}{L}\theta\right) + I_{YY}\cos^2\left(\frac{r}{L}\theta\right) \quad (8b)$$

$$I_{xy}(r) = (I_{YY} - I_{XX})\sin\left(\frac{r}{L}\theta\right)\cos\left(\frac{r}{L}\theta\right) \quad (8c)$$

where

$$I_{XX} = \frac{b_0 t_0^3}{12}\left(1-\alpha\frac{r}{L}\right)\left(1-\beta\frac{r}{L}\right)^3 \quad (9a)$$

$$I_{YY} = \frac{b_0^3 t_0}{12}\left(1-\alpha\frac{r}{L}\right)^3\left(1-\beta\frac{r}{L}\right) \quad (9b)$$

In conducting the present stability analysis, the rotational speed Ω_0 is considered to be perturbed with a small perturbation speed of $f(t)$. Hence,

$$\Omega(t) = \Omega_0 + f(t) \quad (10)$$

If the speed Ω_0 is much smaller than the first natural frequency of the longitudinal vibration of the corresponding stationary beam, the centrifugal force p^* can be approximated as a steady force [19,26], i.e.,

$$p^* = \int_r^L \rho A\Omega_0^2(r + R_h)\,\mathrm{d}r \quad (11)$$

From Hamilton's principle, the equations of motion of the sth blade can then be expressed as

$$\rho A\ddot{u}_s - \rho\Omega_0^2\left[\int_r^L A(r+R_h)\,\mathrm{d}r\,u_s'\right]' + E(I_{yy}u_s'' + I_{xy}v_s'')'' = 0 \tag{12a}$$

$$\begin{aligned}\rho A\ddot{v}_s - \rho\Omega_0^2\left\{Av_s + \left[\int_r^L A(r+R_h)\,\mathrm{d}r\,v_s'\right]'\right\} + E(I_{xx}v_s'' \\ + I_{xy}u_s'')'' + (k_{s+1}+k_s)v_s\delta(r-r_c) - k_{s+1}v_{s+1}\delta(r-r_c) \\ - k_s v_{s-1}\delta(r-r_c) = \rho A(2\Omega_0 f + f^2)v_s \\ \text{for} \quad s = 1, 2, \ldots, N\end{aligned} \tag{12b}$$

where $\delta(r-r_c)$ is the delta function.

The corresponding boundary conditions are given by

$$u_s = v_s = u_s' = v_s' = 0, \quad \text{at} \quad r = 0 \tag{13a}$$

$$u_s'' = v_s'' = u_s''' = v_s''' = 0, \quad \text{at} \quad r = L \tag{13b}$$

The solutions for Eqs. (12a) and (12b) are assumed to be

$$u_s(r,t) = \sum_{i=1}^{m} p_i^s(t)\phi_i^s(r) \tag{14a}$$

$$v_s(r,t) = \sum_{i=1}^{m} q_i^s(t)\phi_i^s(r) \tag{14b}$$

where $p_i^s(t)$ and $q_i^s(t)$ are coefficients to be determined and $\phi_i^s(r)$ are comparison functions.

For reasons of simplicity, two nondimensional variables, $\bar{r} = r/L$ and $\bar{r}_c = r_c/L$, are introduced. This study employs the bending modes of the pretwisted taper beam derived by Lee [27] to approximate the comparison functions. By applying Galerkin's method, the equations of motion of the sth blade, i.e., Eqs. (12a) and (12b), can then be approximated in matrix form as follows:

$$\begin{aligned}[m]_s\begin{Bmatrix}\ddot{p}\\ \ddot{q}\end{Bmatrix}_s + [k]_s\begin{Bmatrix}p\\ q\end{Bmatrix}_s - k_s[\Lambda^{s-1}]\begin{Bmatrix}p\\ q\end{Bmatrix}_{s-1} + (k_{s+1}+k_s)[\Lambda^s]\begin{Bmatrix}p\\ q\end{Bmatrix}_s \\ - k_{s+1}[\Lambda^{s+1}]\begin{Bmatrix}p\\ q\end{Bmatrix}_{s+1} = (2\Omega_0 f + f^2)[d]_s\begin{Bmatrix}p\\ q\end{Bmatrix}_s\end{aligned} \tag{15}$$

where the matrices are of the form

$$[m]_s = \begin{bmatrix}[m]^{uu} & 0\\ 0 & [m]^{vv}\end{bmatrix}_s \tag{16a}$$

$$[k]_s = \begin{bmatrix}[k^e]^{uu} + [k^\Omega]^{uu} & [k^e]^{uv}\\ [k^e]^{uv} & [k^e]^{vv} + [k^\Omega]^{vv}\end{bmatrix}_s \tag{16b}$$

$$[d]_s = \begin{bmatrix}0 & 0\\ 0 & [d]^{vv}\end{bmatrix}_s \tag{16c}$$

where the matrices $[m]_s$, $[k]_s$, and $[d]_s$ are the mass, stiffness, and perturbation matrices, respectively. It is noted that in the present case, the disturbance component matrix $[d]^{vv}$ is identical to the component mass matrix $[m]^{vv}$. The superscripts uu and vv denote components related to the rotational direction and out-off plane direction, respectively, while the superscript uv denotes components which are introduced by the coupling effect. In the stiffness matrices, the superscripts e and Ω relate to the elastic deformation and rotational speed, respectively.

For convenience, the same comparison functions are employed for all blades having no cracks. The matrices $[\Lambda^{s-1}]$, $[\Lambda^s]$, and $[\Lambda^{s+1}]$ are identical for all noncracked blades, and are expressed as

$$[\Lambda^{s-1}] = [\Lambda^s] = [\Lambda^{s+1}] = [\Lambda] \tag{17}$$

and

$$[\Lambda] = \begin{bmatrix}0 & 0\\ 0 & \{\phi\}_s\{\phi\}_s^T\end{bmatrix}\Bigg|_{\bar{r}=\bar{r}} \tag{18}$$

with

$$[\phi(\bar{r})]_s = [\phi_1^s(\bar{r}),\ \phi_2^s(\bar{r}), \ldots, \phi_m^s(\bar{r})]^T$$

B. Blades with Crack

A number of studies [28–30] have explored the effects of cracks on the dynamic and static behaviors of structures. Some investigations [31,32] have considered the effects of cracks in rotating machinery. Under the conditions when a crack is located at $\bar{r} = \bar{r}^*$ of the ξth blade, the cracked shrouded bladed disk assembly can be regarded as a mistuned periodical system. In addition to the strain energy introduced by the bending moment, rotational speed, and shroud deformation, the total strain energy of the ξth defective blade also includes a released energy component U_ξ^c caused by the presence of a crack. Hence,

$$U_\xi = U_\xi^e + U_\xi^\Omega + U_\xi^k - U_\xi^c \tag{19}$$

where U_ξ^c is the released energy introduced from mode I loading.

According to the investigations of Dimarogonas et al. [33,34], the released energy of a crack can be approximated as

$$U_\xi^c = b_0(1-\alpha\bar{r}^*)\int_0^a \frac{(1-\mu^2)}{E}K_I^2\,\mathrm{d}a \tag{20}$$

where a and μ are the depth of the crack and the Poisson's ratio of the blade, respectively, and K_I is a stress intensity factor, which can be estimated from the equation proposed by Tada et al. [30], i.e.,

$$K_I = \frac{6p_b}{t_0^2 b_0(1-\alpha\bar{r}^*)(1-\beta\bar{r}^*)^2}\sqrt{\pi\bar{\gamma}t_0(1-\beta\bar{r}^*)}\,F_I(\bar{\gamma}) \tag{21}$$

where the variables for a near root crack can be approximated as

$$p_b = EI_{xx}v_\xi''|_{\bar{r}=\bar{r}^*} \quad \text{and} \quad \bar{\gamma} = \frac{a}{t_0(1-\beta\bar{r}^*)} \tag{22}$$

$$F_I(\bar{\gamma}) = \sqrt{\frac{2}{\pi\bar{\gamma}}\tan\left(\frac{\pi\bar{\gamma}}{2}\right)}\frac{0.923 + 0.199[1-\sin(\pi\bar{\gamma}/2)]^4}{\cos(\pi\bar{\gamma}/2)} \tag{23}$$

Equation (20) can be modified to the following form:

$$U_\xi^c = 3E(1-\mu^2)t_0(1-\beta\bar{r}^*)\int_0^1 I_{xx}Q(\bar{\gamma})(v_\xi'')^2\delta(\bar{r}-\bar{r}^*)\,\mathrm{d}\bar{r} \tag{24}$$

and

$$Q(\bar{\gamma}) = \int_0^{\bar{\gamma}} \pi\bar{\gamma}F_I^2(\bar{\gamma})\,\mathrm{d}\bar{\gamma} \tag{25}$$

Similarly, the equation of motion of the ξth cracked blade can be rewritten in matrix form as

$$\begin{aligned}[m]_\xi\begin{Bmatrix}\ddot{p}\\ \ddot{q}\end{Bmatrix}_\xi + [k]_\xi\begin{Bmatrix}p\\ q\end{Bmatrix}_\xi - k_\xi[\Lambda^{\xi-1}]\begin{Bmatrix}p\\ q\end{Bmatrix}_{\xi-1} + (k_{\xi+1}+k_\xi)[\Lambda^\xi]\begin{Bmatrix}p\\ q\end{Bmatrix}_\xi \\ - k_{\xi+1}[\Lambda^{\xi+1}]\begin{Bmatrix}p\\ q\end{Bmatrix}_{\xi+1} = (2\Omega_0 f + f^2)[d]_\xi\begin{Bmatrix}p\\ q\end{Bmatrix}_\xi\end{aligned} \tag{26}$$

where

$$[k]_\xi = \begin{bmatrix}[k^e]^{uu} + [k^\Omega]^{uu} & [k^e]^{uv}\\ [k^e]^{uv} & [k^e]^{vv} + [k^\Omega]^{vv} - [k^{cv}]\end{bmatrix}_\xi \tag{27}$$

The stiffness matrix $[k^{cv}]$ introduced by the crack is given by

$$k_{ij}^{cv} = 6\frac{EI_{xx}}{L^4}(1-\mu^2)\left(\frac{t_0}{L}\right)(1-\beta\bar{r}^*)Q(\bar{\gamma})[\phi_i''(\bar{r})\phi_j''(\bar{r})]_{\bar{r}=\bar{r}^*} \quad (28)$$

C. Equation of Motion of Bladed Disk Assembly

The equation of motion of the complete rotating bladed disk assembly can be grouped as

$$[M]\{\ddot{X}\} + [K]\{X\} = (2\Omega_0 f + f^2)[D]\{X\} \quad (29)$$

The system stiffness matrix $[K]$ is given by

$$[K] = \begin{bmatrix} [\alpha]_1 & -k_2[\Lambda] & 0 & . & 0 & 0 & -k_1[\Lambda] \\ -k_2[\Lambda] & [\alpha]_2 & -k_3[\Lambda] & . & 0 & 0 & 0 \\ 0 & -k_3[\Lambda] & [\alpha]_3 & . & 0 & 0 & 0 \\ . & . & . & . & . & . & . \\ 0 & 0 & 0 & . & [\alpha]_{N-2} & -k_{N-1}[\Lambda] & 0 \\ 0 & 0 & 0 & . & -k_{N-1}[\Lambda] & [\alpha]_{N-1} & -k_N[\Lambda] \\ -k_1[\Lambda] & 0 & 0 & . & 0 & -k_N[\Lambda] & [\alpha]_N \end{bmatrix} \quad (30)$$

$$\{X\} = \left[\begin{Bmatrix} p \\ q \end{Bmatrix}_1^T, \begin{Bmatrix} p \\ q \end{Bmatrix}_2^T, \ldots, \begin{Bmatrix} p \\ q \end{Bmatrix}_{N-1}^T, \begin{Bmatrix} p \\ q \end{Bmatrix}_N^T\right]^T \quad (31)$$

and

$$[\alpha]_s = [k]_s + k_{s+1}[\Lambda] + k_s[\Lambda] \quad \text{for} \quad s = 1, 2, 3, \ldots, N \quad (32)$$

The cyclic arrangement of the N blades of the bladed disk assembly implies that

$$\begin{Bmatrix} p \\ q \end{Bmatrix}_{N+1} = \begin{Bmatrix} p \\ q \end{Bmatrix}_1 \quad \text{and} \quad k_1 = k_{N+1} \quad (33)$$

III. Analysis of Cracked Bladed Disk Assembly

Let $[\Psi]$ be the normalized modal matrix of the corresponding eigenvalue problem of Eq. (29). Hence,

$$[\Psi]^T[M][\Psi] = [I] = \begin{bmatrix} 1 & 0 & 0 & \cdots & 0 \\ 0 & 1 & 0 & \cdots & 0 \\ \vdots & & \ddots & & \vdots \\ 0 & & 0 & 0 & 1 \end{bmatrix} \quad (34)$$

and

$$[\Psi]^T[K][\Psi] = [A] = \begin{bmatrix} \omega_1^2 & 0 & 0 & \cdots & 0 \\ 0 & \omega_2^2 & 0 & \cdots & 0 \\ \vdots & & \ddots & & \vdots \\ 0 & 0 & 0 & & \omega_N^2 \end{bmatrix} \quad (35)$$

where $\omega_1^2, \omega_2^2, \ldots, \omega_N^2$ are the eigenvalues of the cracked bladed disk assembly.

From the expansion theorem, the response can be approximated as

$$\{X\} = [\Psi]\{u\} \quad (36)$$

Equation (29) can then be rewritten as

$$[I]\{\ddot{u}\} + [A]\{u\} = -\left(\frac{f}{\Omega_0} + \frac{f^2}{2\Omega_0^2}\right)[D]^*\{u\} \quad (37)$$

where

$$[D]^* = -2\Omega_0^2[\Psi]^T[D][\Psi] \quad (38)$$

Let the rotational speed be perturbed by a very small periodic excitation $f(t)$, which can be represented by a Fourier series of harmonic components as

$$f(t) = \sum_{j=-Q}^{Q} F_j e^{i\omega_j t} \quad (39)$$

where ω_j is the jth harmonic frequency.

Substituting Eq. (39) into Eq. (37), the dynamic equation of the cracked blade assembly can be rewritten as

$$[I]\{\ddot{u}\} + [A]\{u\} = -\varepsilon\left(\bar{f} + \frac{\varepsilon}{2}\bar{f}^2\right)[D]^*\{u\} \quad (40)$$

with

$$\varepsilon = \frac{|F_M|}{\Omega_0} \quad \text{and} \quad \bar{f}(t) = \frac{f(t)}{|F_M|}$$

where ε is the relative disturbance order and $|F_M|$ is the maximum magnitude of components F_j for $j = 1, 2, \ldots, Q$.

Under the current assumption that the magnitude of the speed variation $f(t)$ is very small, the ratio ε is less than one. Equation (40) represents a set of N uncoupled differential equations of the type

$$\ddot{u}_n + \omega_n^2 u_n = -\varepsilon\left(\bar{f} + \frac{\varepsilon}{2}\bar{f}^2\right)\sum_{m=1}^{N} \mathrm{d}_{nm}^* u_m \quad \text{for} \quad n = 1, 2, 3, \ldots, N \quad (41)$$

where d_{nm}^* is the element of matrix $[D]^*$.

Using the multiple scales method, a series of new independent variables are introduced, namely $T_\alpha = \varepsilon^\alpha t$ for $(\alpha = 0, 1, 2, \ldots)$. It follows that the derivatives with respect to t are given by:

$$\frac{\mathrm{d}}{\mathrm{d}t} = \frac{\mathrm{d}T_0}{\mathrm{d}t}\frac{\partial}{\partial T_0} + \frac{\mathrm{d}T_1}{\mathrm{d}t}\frac{\partial}{\partial T_1} + \cdots = D_0 + \varepsilon D_1 + \cdots \quad (42)$$

$$\frac{\mathrm{d}^2}{\mathrm{d}t^2} = D_0^2 + 2\varepsilon D_0 D_1 + \varepsilon^2(D_1^2 + 2D_0 D_2) + \cdots \quad (43)$$

The solution of Eq. (41) can then be represented by an expansion form, i.e.,

$$u_n(t;\varepsilon) = u_{n0}(T_0, T_1, T_2, \ldots) + \varepsilon^1 u_{n1}(T_0, T_1, T_2, \ldots) \quad (44)$$

Substituting Eqs. (42–44) into Eq. (41), and collecting terms in powers of $\varepsilon^0, \varepsilon^1, \varepsilon^2, \ldots$, yields the following equations:

$$\text{order} \quad \varepsilon^0 \quad D_0^2 u_{n0} + \omega_n^2 u_{n0} = 0 \quad (45a)$$

$$\text{order} \quad \varepsilon^1 \quad D_0^2 u_{n1} + \omega_n^2 u_{n1} = -2D_0 D_1 u_{n0} - \bar{f}\sum_{r=1}^{N} \mathrm{d}_{nr}^* u_{r0} \quad (45b)$$

Because of the complexity of the equations of motion and the marginal difference between the first and second order approximation results [19,20], this study chooses not to perform the second order expansion. Based on the first order approximation solution, the general solution of Eq. (45a) can be written as

$$u_{n0} = A_n(T_1, T_2)\exp(i\omega_n T_0) + \text{c.c.} \quad (46)$$

where $A_n(T_1, T_2)$ is an unknown complex function.

For simplicity, the periodic speed perturbation is assumed to have the form

$$\bar{f} = \sum_{j=1}^{Q} \hat{F}_j \, e^{i\omega_j t} + \text{c.c.} \tag{47}$$

Substituting the general solution of Eq. (46) into Eq. (45b) yields

$$D_0^2 u_{n1} + \omega_n^2 u_{n1} = -2i\omega_n (D_1 A_n) e^{i\omega_n T_0} - \sum_{j=1}^{Q} \hat{F}_j \sum_{r=1}^{N} \mathrm{d}_{nr}^* \{A_r e^{i[\omega_r + \omega_j]T_0} + \bar{A}_r e^{i[\omega_r - \omega_j]T_0}\} + \text{c.c.} \tag{48}$$

where $\bar{A}_r$ denotes the complex conjugate of A_r.

The complex coefficient A_n is to be determined in such a way as to eliminate the problematic terms from u_{n1}. The choice depends upon the particular resonant combinations of the frequencies. This study considers four cases [17,19].

A. When ω_j is Located away from Frequencies ($\omega_p \pm \omega_q$)

As noted, the existence of the term $-2i\bar{\omega}_n (D_1 A_n) e^{i\bar{\omega}_n T_0}$ in Eq. (48) may cause difficulties when attempting to establish the particular solutions. The problematic terms are eliminated if

$$A_n = A_n(T_2) \quad \text{therefore} \quad D_1 A_n = 0 \tag{49}$$

The particular solution u_{n1} can then be solved as

$$u_{n1} = \sum_{j=1}^{Q} \hat{F}_j \sum_{r=1}^{N} \mathrm{d}_{nr}^* A_r \left\{ \frac{\exp[i(\omega_r + \omega_j)T_0]}{(\omega_r + \omega_j)^2 - \omega_n^2} + \frac{\exp[i(\omega_j - \omega_r)T_0]}{(\omega_j - \omega_r)^2 - \omega_n^2} \right\} + \text{c.c.} \tag{50}$$

This solution reveals that the shrouded bladed disk assembly remains stable in this particular case.

B. When $\omega_j \to (\omega_p + \omega_q)$

In this so-called combination resonance of the summed type case, it is assumed that

$$\bar{\omega}_j = \bar{\omega}_p + \bar{\omega}_q + \varepsilon\sigma \tag{51}$$

where σ is the detuning parameter.

Hence,

$$(\bar{\omega}_j - \bar{\omega}_q)T_0 = \bar{\omega}_p T_0 + \sigma T_1 \tag{52a}$$

$$(\bar{\omega}_j - \bar{\omega}_p)T_0 = \bar{\omega}_q T_0 + \sigma T_1 \tag{52b}$$

Substituting Eqs. (52a) and (52b) into Eq. (48), it leads to

$$A_p = a_p \exp(-i\lambda T_1) \tag{53a}$$

$$A_q = a_q \exp[i(\bar{\lambda} + \sigma)T_1] \tag{53b}$$

where a_p and a_q are complex functions of T_2 and $\bar{\lambda}$ is the complex conjugate of λ.

Equations (48), (53a), and (53b) can be used to locate the stability boundaries, which are defined by the imaginary part of λ . The shrouded bladed disk assembly is stable when the imaginary part of λ is negative, but an unstable flutter occurs when the imaginary part of λ is positive. The solutions, i.e., A_p and A_q, are bounded when the system is stable. The transition curves between the stable and unstable zones can be derived as

$$\omega_j = \omega_p + \omega_q \pm \varepsilon \sqrt{\sum_{j=1}^{Q} \hat{F}_j^2 \Lambda_{pq}} \tag{54}$$

where $\Lambda_{pq} = (d_{pq}^* d_{qp}^*)/(\omega_p \omega_q)$.

When $p = q$, the preceding equation is reduced to the Mathieu equation.

$$\omega_j = 2\omega_p \pm \varepsilon \sum_{j=1}^{Q} \hat{F}_j \frac{d_{pp}^*}{\omega_p} \tag{55}$$

C. When $\omega_j \to (\omega_p - \omega_q)$

As mentioned in the preceding case, the transition curves of resonant combinations are given by

$$\omega_j = \omega_p - \omega_q \pm \varepsilon \sqrt{-\sum_{j=1}^{Q} \hat{F}_j^2 \Lambda_{pq}} \tag{56}$$

However, this case occurs only when d_{pq}^* and d_{qp}^* have opposing mathematical signs.

D. When $\omega_j \to (\omega_p + \omega_q)$ and $(\omega_q + \omega_s)$

In a special case, the perturbation frequency ω_j approaches the resonant combinations $\omega_p + \omega_q$ and $\omega_q + \omega_s$ simultaneously. In this situation, the transition curves are amended by changing the relationship of the detuning parameter to

$$\bar{\omega}_j = \bar{\omega}_p + \bar{\omega}_q + \varepsilon\sigma_1 \tag{57a}$$

$$\bar{\omega}_j = \bar{\omega}_q + \bar{\omega}_s + \varepsilon\sigma_2 \tag{57b}$$

Substituting Eqs. (57a) and (57b) into Eq. (48) and setting $n = p = q = s$ yields the following nontrivial solutions:

$$A_q = a_q \exp(i\lambda T_2) \tag{58a}$$

$$A_s = a_s \exp[i(\bar{\lambda} + \sigma_2)T_2] \tag{58b}$$

$$A_p = a_p \exp[i(\bar{\lambda} + \sigma_1)T_2] \tag{58c}$$

From Eqs. (58a–58c) and (48), the stability boundary equations of the system can be derived as

$$\lambda^3 + (\sigma_1 + \sigma_2)\lambda^2 + \left(\sigma_1\sigma_2 + \frac{1}{4}(\Lambda_{qs} + \Lambda_{pq}) \sum_{j=1}^{Q} \hat{F}_j^2\right)\lambda + \frac{1}{4}(\sigma_1 \Lambda_{qs} + \sigma_2 \Lambda_{pq}) \sum_{j=1}^{Q} \hat{F}_j^2 = 0 \tag{59}$$

where

$$\sigma_1 = \frac{\omega_j - \omega_p - \omega_q}{\varepsilon} \quad \text{and} \quad \sigma_2 = \frac{\omega_j - \omega_p - \omega_s}{\varepsilon}$$

Equation (59) is a cubic equation for λ and has closed-form solutions. The transition curves can be determined using the value of ω_j for which λ has two real roots.

IV. Numerical Results and Discussion

Some studies [35,36] focus on the dynamic characteristics in blade-shaft system. However, in the present simulations, the bladed disk assembly was considered to consist of 46 pretwisted taper beams attached to a rigid hub, as shown in Fig. 1a. A shroud spring k_s was attached between the tips of neighboring blades. The blades were specified with the following nondimensional parameters: $(R_h/L) = 0.2$, $(b_o/L) = 0.1$, $(t_0/L) = 0.02$, $\alpha = \beta = 0.25$, $\theta = 45°$, and $\bar{r}^* = 0$. For convenience, a number of nondimensional parameters were also adopted, i.e., $\bar{\omega} = \omega/\omega_0$, $\bar{\omega}_n = \omega_n/\omega_0$, $\bar{\Omega}_0 = \Omega_0/\omega_0$, and $\bar{k}_s = (12k_s L^3)/Eb_0 t_0^3$, where ω_n is the natural frequency of the shrouded bladed assembly and ω_0 is a reference frequency defined as $\omega_0 = 0.01\sqrt{E/\rho L^2}$. As a crack propagates on a

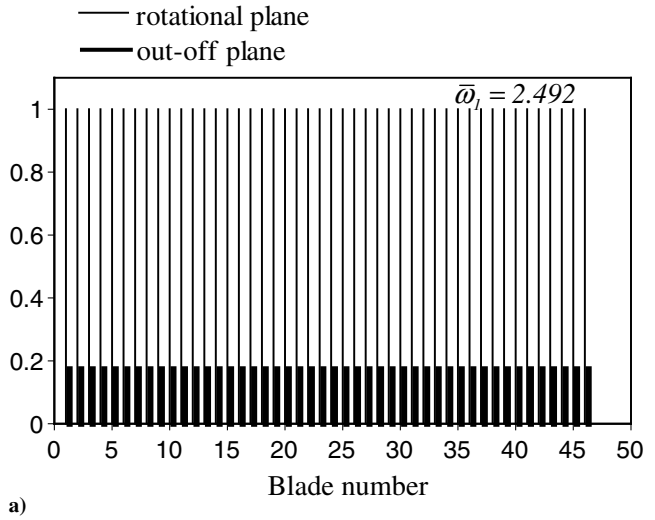

a)

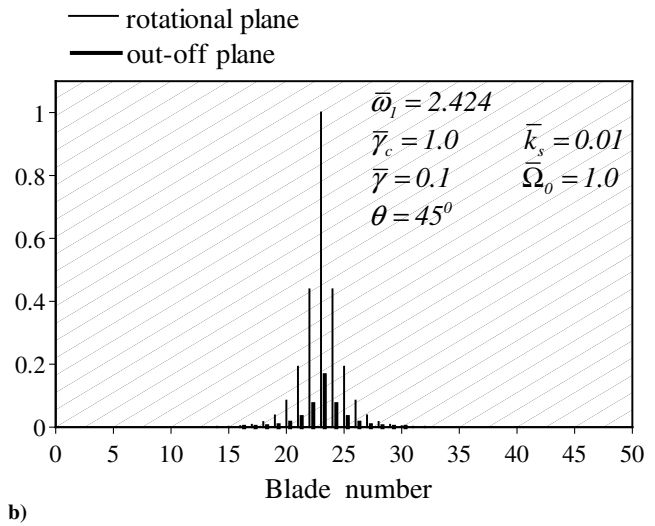

b)

Fig. 2 Tip amplitude patterns of cracked bladed disk assembly: a) no crack (the 1st mode), and b) with a crack $\bar{\gamma} = 0.1$ (the 1st mode).

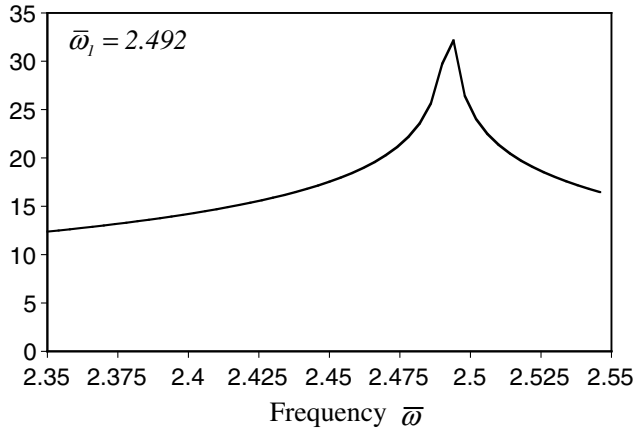

a)

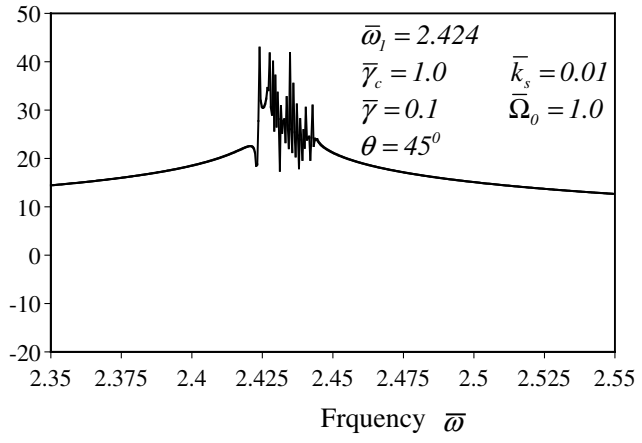

b)

Fig. 3 Tip frequency response at tip of 23rd blade: a) no crack, and b) with a crack $\bar{\gamma} = 0.1$.

blade, it introduces the so-called modal localization phenomenon throughout the entire bladed disk assembly. The amplitudes of the individual defective blades in turn are significantly excited at the localization frequency, i.e., the lowest natural frequency. This study investigates the stability variations introduced by a near root local crack. For simplicity, the study considers the case of a single crack located at the root of the 23rd blade. The stability effects of the crack depth, a, shroud stiffness, k_s, and rotational speed of the blade, Ω_0, are studied.

Before considering the dynamic instability of the cracked bladed disk assembly, it is appropriate to illustrate the characteristics of this system. Figures 2a and 2b present the blade tip displacement patterns of the shrouded bladed disk assembly at the local frequency with and without a local crack, respectively. It is noted that the figures show the blade tip amplitude distributions in both the rotational and out-off rotational planes. As shown in Fig. 2a, a uniform blade tip amplitude distribution occurs when there are no cracks within the bladed disk assembly. However, from Fig. 2b, it can be seen that the presence of a crack near the root of the 23rd blade induces a severe vibration effect in the neighboring blades. Figure 2b illustrates the so-called mode localization phenomenon, which occurs in a periodic structural system with a local defect. Figures 3a and 3b indicate the frequency response at the tip of the 23rd blade for the bladed disk assembly with and without a local crack, respectively. In the disk assembly with no blade cracks, the frequencies of all 46 blades in the periodic system are equal, i.e., $\bar{\omega}_1 = \bar{\omega}_2 = \cdots = \bar{\omega}_{46} = 2.492$ and hence, a single peak is noted in the frequency response at $\bar{\omega}_1 = 2.492$. Conversely, Fig. 3b reveals a more complicated frequency spectrum for the system with a single local crack. The results indicate that the lowest frequency, i.e., the localization frequency, reduces from $\bar{\omega}_1 = 2.492$ to $\bar{\omega}_1 = 2.424$. Multiple peaks are observed near this localization frequency. It is clear that the presence of a local crack in the periodic blade assembly has a significant influence on the dynamic characteristics of the system. To determine the stability of a rotating cracked bladed disk assembly, a simplified harmonic perturbation speed of $f(t) = 2\cos\omega t$ is imposed on the steady rotational speed of Ω_0. Figure 4a presents the distribution of the unstable bands of a cracked bladed disk assembly as predicted from the stability analysis described above. The first unstable band is composed of a series of unstable zones near the resonance frequencies ($2\bar{\omega}_1 \sim 2\bar{\omega}_{46}$), as shown in Fig. 4b. The presence of a local crack changes the lowest natural frequencies of all 46 blades in the bladed disk assembly from a uniform value of $\bar{\omega}_1 = \bar{\omega}_2 = \cdots = \bar{\omega}_{46} = 2.492$ to a cluster of distributed resonance frequencies in the range of $\bar{\omega}_1 = 2.333$ to $\bar{\omega}_{46} = 2.370$. As shown in Fig. 3b, the modal localization phenomenon introduced by a local crack changes the dynamic characteristics near the localization frequency. This variation in the dynamic characteristics changes the distribution of the unstable zones near the resonant frequencies, as shown in Fig. 4a. The stability analysis of the cracked bladed disk assembly also reveals the presence of a series of small stable regions near the resonant frequencies ($2\bar{\omega}_1 \sim 2\bar{\omega}_{46}$), as shown in Fig. 4b. However, these very small stable regions distributed in the frequency band ($2\bar{\omega}_1 \sim 2\bar{\omega}_{46}$) have negligible impact upon the system. The unstable zones related to resonant frequencies ($2\bar{\omega}_1, 2\bar{\omega}_2, \ldots, 2\bar{\omega}_{46}$), are located so close to each other that they can barely be separated.

Figures 5a and 5b demonstrate the influence of the crack depth upon the variations in the transition curves. The results indicate that

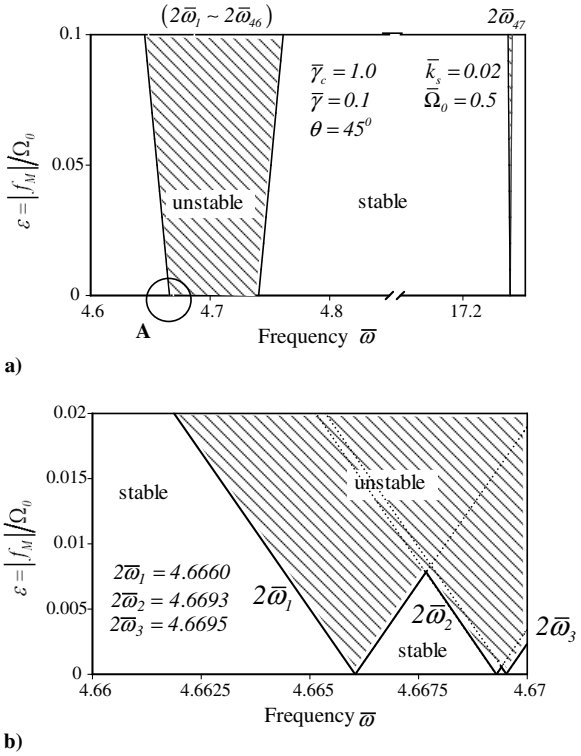

Fig. 4 Transition curves for cracked bladed disk assembly: a) regions of instability, and b) detail for zone A.

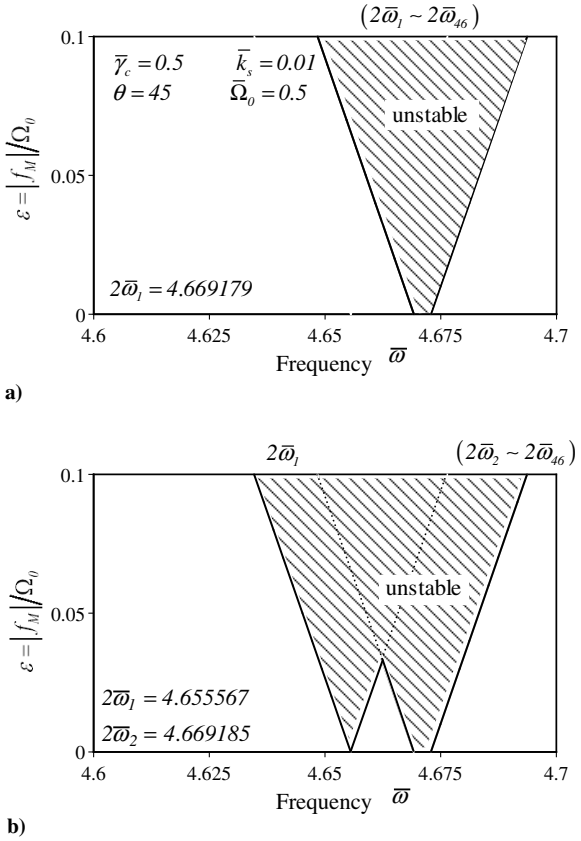

Fig. 5 Variations in transition curves for different crack depths: a) without cracks $\bar{\gamma} = 0.0$, and b) crack $\bar{\gamma} = 0.1$.

the unstable zone near $2\bar{\omega}_1$ is shifted to the left as the depth of the crack in the 23rd blade is increased from $\bar{\gamma} = 0.01$ to $\bar{\gamma} = 0.1$. As noted by Kuang and Huang [13], increasing the crack depth enhances the modal localization phenomenon and reduces the localization frequency $2\bar{\omega}_1$. As shown in Fig. 5b, the current localization frequency shift from $2\bar{\omega}_1 = 4.669$ to $2\bar{\omega}_1 = 4.656$ enlarges the unstable band.

The rotational speed of the blades $\bar{\Omega}_0$ also affects the unstable bands, as shown in Figs. 6a and 6b. The additional stiffness introduced by the centrifugal force increases the natural frequencies. It can be observed that the first unstable band is enlarged and shifted toward a higher frequency of $2\bar{\omega}_1 = 4.8507$ as the rotational speed is increased to $\bar{\Omega}_0 = 1.0$. Previous researchers [5,6] have reported that the degree of localization depends significantly upon the magnitude of the disorder and the modal coupling effect. The modal coupling effect in the current periodic bladed disk assembly is dominated by the spring constant of the shroud $\bar{k}_s$. For a mistuned system, strong localization occurs in a weakly coupled system [37]. The effect of shroud stiffness on the stability of the present bladed disk assembly is shown in Figs. 7a and 7b. It is observed that the unstable bands are significantly enlarged as the coupling stiffness is increased from $\bar{k}_s = 0.02$ to $\bar{k}_s = 0.1$.

V. Conclusions

The present study has demonstrated that the stability of a rotating periodic shrouded bladed disk assembly is sensitive to the presence of local blade cracks. In general, the modal localization phenomenon caused by the local crack defect does not only change the dynamic responses of the system at the lowest natural frequency, but also influences the unstable band significantly. The major conclusions to be drawn from the present analysis and discussions are summarized as follows:

1) The present stability analysis indicates that the localization effect generates a series of closely spaced unstable zones. These instability zones enlarge as the interblade coupling stiffness is increased. Although higher shroud stiffness between adjacent blades may reduce the mode localization phenomenon, it enlarges the

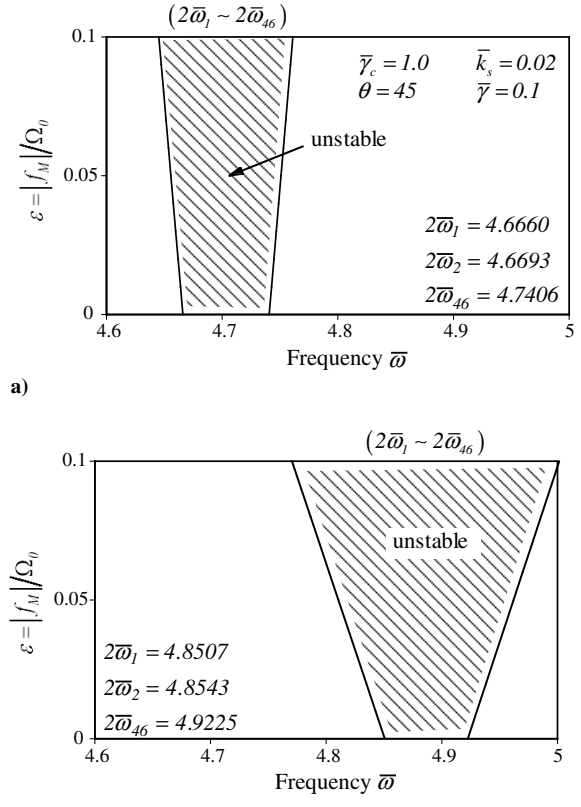

Fig. 6 Variations in transition curves for different rotating speeds: a) speed at $\bar{\Omega}_0 = 0.5$, and b) speed at $\bar{\Omega}_0 = 1.0$.

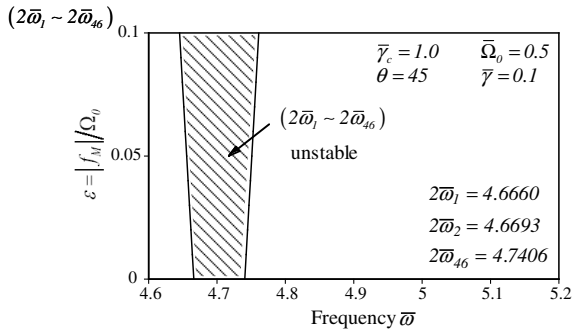

a)

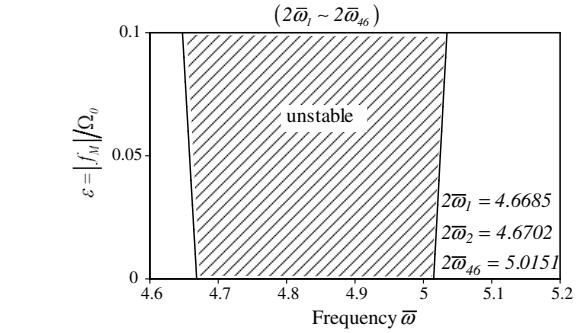

b)

Fig. 7 Variations in transition curves for different coupling stiffness: a) shroud stiffness at $\bar{k}_s = 0.02$, and b) shroud stiffness at $\bar{k}_s = 0.1$.

instability region and hence, destabilizes the cracked disk assembly system.

2) The depth of the local crack has a fundamental effect on the stability of a rotating mistuned bladed disk assembly. The present results indicate that the first unstable zone is enlarged as the depth of the crack is increased.

3) The results show that the rotational speed of a cracked bladed disk assembly has a significant influence on its instability behavior. Specifically, a higher rotation speed shifts the unstable zone toward a higher frequency region.

Acknowledgment

The authors gratefully acknowledge the support provided to this study by the National Science Council under Grant No. NSC88-TPC-7-110-01.

References

[1] Bernstein, H. L., and Alien, J. M., "Analysis of Cracked Gas Turbine Blades," *Journal of Engineering for Gas Turbines and Power*, Vol. 114, April 1992, pp. 293–301.

[2] Walls, D. P., deLaneuville, R. E., and Cunningham, S. E., "Damage Tolerance Based Life Prediction in Gas Turbine Engine Blades under Vibratory High Cycle Fatigue," *Journal of Engineering for Gas Turbines and Power*, Vol. 119, Jan. 1997, pp. 143–146.

[3] Bendiksen, O. O., "Modal Localization Phenomena in Large Space Structures," *AIAA Journal*, Vol. 25, No. 9, 1987, pp. 1241–1248.

[4] Hodges, C. H., "Confinement of Vibration by Structural Irregularity," *Journal of Sound and Vibration*, Vol. 82, No. 3, 1982, pp. 411–424.

[5] Wei, S. T., and Pierre, C., "Localization Phenomena in Mistuned Assemblies with Cyclic Symmetry Part I: Free Vibrations," *Journal of Vibration, Acoustics, Stress, and Reliability in Design*, Vol. 110, Oct. 1988, pp. 429–438.

[6] Wei, S. T., and Pierre, C., "Localization Phenomena in Mistuned Assemblies with Cyclic Symmetry Part II: Forced Vibrations," *Journal of Vibration, Acoustics, Stress, and Reliability in Design*, Vol. 110, Oct. 1988, pp. 439–449.

[7] Orgun, C. O., and Tongue, B. H., "Modal Localization in Coupled Circular Plates," *Journal of Vibration and Acoustics*, Vol. 116, July 1994, pp. 286–294.

[8] Huang, B. W., and Kuang, J. H., "Mode Localization in a Rotating Mistuned Turbo Disk with Coriolis Effect" *International Journal of Mechanical Sciences*, Vol. 43, No. 7, 2001, pp. 1643–1660.

[9] Cottney, D. J., and Ewins, D. J., "Towards the Efficient Vibration Analysis of Shrouded Bladed Disk Assemblies," *Journal of Engineering for Industry*, Vol. 96B, 1974, pp. 1054–1059.

[10] Afolabi, D., "The Eigenvalue Spectrum of Mistuned Bladed Disk," *Vibrations of Blades and Bladed Disk Assemblies, Proceedings of the Tenth Biennial Conference on Mechanical Vibration and Noise*, 1985, pp. 15–22.

[11] Basu, P., and Griffin, J. H., "The Effect of Limiting Aerodynamic and Structural Coupling in Models of Mistuned Blade Disk Vibration," *Journal of Vibration, Acoustics, Stress, and Reliability in Design*, Vol. 108, April 1985, pp. 132–139.

[12] Kaneko, Y., Mase, M., Fujita, K., and Nagashima, T., "Vibration Response Analysis of Mistuned Bladed Disk," *JSME International Journal Series C*, Vol. 37, No. 1, 1994, pp. 33–40.

[13] Kuang, J. H., and Huang, B. W., "Mode Localization on a Cracked Bladed Disk," *Journal of Engineering for Gas Turbines and Power*, Vol. 121, No. 2, 1999, pp. 335–342.

[14] Huang, B. W., and Kuang, J. H., "The Effect of Local Crack on the Dynamic Characteristics of a Rotating Grouped Bladed Disk," *Journal of Mechanical Engineering Science*, Vol. 216, No. 4, 2002, pp. 447–457.

[15] Rao, J. S., "Flexural Vibration of Pretwisted Tapered Cantilever Blades," *Journal of Engineering for Industry*, Vol. 94, No. 1, Feb. 1972, pp. 343–346.

[16] Rao, J. S., "Vibration of Rotating, Pretwisted, and Tapered Blades," *Mechanism and Machine Theory*, Vol. 12, No. 2, 1977, pp. 331–337.

[17] Nayfey, A. H., and Mook, D. T., *Nonlinear Oscillation*, Wiley, New York, 1979, pp. 304–310.

[18] Hsu, C. S., "On a Restricted Class of Coupled Hill's Equations and Some Applications," *Journal of Applied Mechanics*, Jan. 1961, pp. 551–557.

[19] Young, T. H., "Dynamic Response of a Pretwisted, Tapered Beam with Non-Constant Rotating Speed," *Journal of Sound and Vibration*, Vol. 150, No. 3, 1991, pp. 435–446.

[20] Liao, C. L., and Huang, B. W., "Parametric Resonance of a Spinning Pretwisted Beam with Time-Dependent Spinning Rate," *Journal of Sound and Vibration*, Vol. 180, No. 1, 1995, pp. 47–65.

[21] Ng, T. Y., Lam, K. Y., and Li, H., "Dynamic Stability of Rotating Blades with Transverse Cracks," *Shock and Vibration*, Vol. 10, No. 3, 2003, pp. 187–194.

[22] Lin, C. Y., and Chen, L. W., "Dynamic Stability of Rotating Pre-Twisted Blades with a Constrained Damping Layer," *Composite Structures*, Vol. 61, No. 3, 2003, pp. 235–245.

[23] Sakar, G., and Sabuncu, M., "Dynamic Stability of a Rotating Asymmetric Cross-Section Blade Subjected to an Axial Periodic Force," *International Journal of Mechanical Sciences*, Vol. 45, No. 9, 2003, pp. 1467–1482.

[24] Sakar, G., and Mustafa, S., "Buckling and Dynamic Stability of a Rotating Pretwisted Asymmetric Cross-Section Blade Subjected to an Axial Periodic Force," *Finite Elements in Analysis and Design*, Vol. 40, No. 11, 2004, pp. 1399–1415.

[25] Bendiksen, O. O., "Flutter of Mistuned Turbo Machinery Rotors," *Journal of Engineering for Gas Turbines and Power*, Vol. 106, Jan. 1984, pp. 23–25.

[26] Anderson, G. L., "On the Extensional and Flexural Vibrations of Rotating Bar," *International Journal of Nonlinear Mechanics*, Vol. 10, 1975, pp. 223–236.

[27] Lee, H. P., "Effects of Axial Base Excitations on the Dynamic Stability of Spinning Pretwisted Cantilever Beams," *Journal of Sound and Vibration*, Vol. 185, No. 2, 1995, pp. 265–278.

[28] Rizos, P. F., Aspragathos, N., and Dimarogonas, A. D., "Identification of Crack Location and Magnitude in a Cantilever Beam from the Vibration Mode," *Journal of Sound and Vibration*, Vol. 138, No. 3, 1990, pp. 381–388.

[29] Broek, D., *Elementary Engineering Fracture Mechanics*, Martinus–Nijhoff, Boston, 1986, pp. 123–146.

[30] Tada, H., Paris, P., and Irwin, G., *The Stress Analysis of Crack Handbook*, Del Research Corp., Hellertown, PA, 1973.

[31] Chen, L., and Chen, C., "Vibration and Stability of Cracked Thick Rotating Blade," *Computers & Structures*, Vol. 28, No. 1, 1988, pp. 67–74.

[32] Grabowski, B., "The Vibrational Behavior of a Turbine Rotor Containing a Transverse Crack," *Journal of Mechanical Design*, Vol. 102, Jan. 1980, pp. 140–146.

[33] Dimarogonas, A. D., and Paipetis, S. A., *Analytical Methods in Rotor Dynamics*, Applied Science Publishers, New York, 1983, pp. 144–159.

[34] Krawczuk, M., and Ostachowicz, W. M., "Transverse Natural Vibrations of a Cracked Beam Loaded with a Constant Axial Force," *Journal of Vibration and Acoustics*, Vol. 115, Oct. 1993, pp. 524–528.
[35] Al-Bedoor, B. O., Ghotti, L., Aidwesi, S., Al-Nassar, Y. N., and Abdelsamad, M., "Experiments on Extracting Blade Vibration using Tensional Vibration Measurement of the Shaft," *Journal of Quality in Maintenance Engineering*, Vol. 9, No. 2, 2003, pp. 144–159.
[36] Al-Nassar, Y. N., and Al-Bedoor, B. O., "On the Vibration of Rotating Blade with Torsionally-Flexible Shaft," *Journal of Sound and Vibration*, Vol. 259, No. 5, 2003, pp. 1237–1242.
[37] Pierre, C., "Weak and Strong Vibration Localization in Disordered Structures: A Statistical Investigation," *Journal of Sound and Vibration*, Vol. 139, No. 1, 1990, pp. 111–132.

C. Pierre
Associate Editor